Supplementary Information

Table S1. Bioinformatics analysis and RNAi-mediated screening of BAR domain containing proteins in *Drosophila.*

Sl. No.	Human BAR domain protein	*Drosophila* orthologs	Overall Sequence identity	RNAi Lines used
1	Arfaptin1/2	CG17184	52%	v103951, v20401
2	ICA69	CG10566	36%	v105120,v27281,BL-28379
3	PICK1	CG6167	60%	v104486, v22268,v22269
4	Amphiphysin 1/2	CG8604	35%	BL-28048
5	Endophilin A1-3	CG14296	49%	BL-27679
6	Endophilin B1/2	CG9834	44%	BL-27537
7	APPL1	CG1363	45%	ND
8	ARHGAP17/44	CG4755	31%	v105663,v34895,v34896
9	Oligophrenin1	CG8948	41%	v110812,v42166,BL-51853
10	ASAP1-3	CG30372	45%	v106932,v19284,BL-31149
11	Tuba	-	-	-
12	ACAP1- 3	CG6742	31%	v27739,v27738,BL-31147
13	SNX1	CG2774	52%	BL-38301
14	SNX5	CG8282	53%	v110170,v24275,BL-38278
15	SNX9	CG6757	33%	BL-27653
16	FER, FES	CG8874	37%	ND
17	PACSIN1-3	CG33094	41%	v104580,BL-27297
18	FCHO1/2	CG8176	35%	BL-63002
19	NOSTRIN	CG42388	54%	ND
20	PSTPIP1	CG33094	22%	-
21	FCHSD1/2	CG43479	25%	BL-27713
22	TOCA1	CG15015	35%	BL-31646
23	FBP17	CG15015	36%	ND
24	ABBA	CG33558	48%	BL-43223
25	BAIAP2L2	CG32082	28%	BL-44526

Human BAR domain containing proteins were first identified from the literature searches. Using these proteins as query sequences, their closest sequences (likely fly orthologs) were identified in annotated *Drosophila* genome sequences (www.flybase.org) and selected based on the identity and similarity of their sequences. *Drosophila* RNAi lines used for knockdown experiments in this study is listed. The RNAi lines were driven with *Actin 5C*-Gal4 driver, and the F1 larval fillets were immunostained with neuronal membrane marker, anti-HRP antibody. NMJ were compared with control larval fillets for any morphological defects. We identified ICA69 as one of the key regulators of NMJ morphology. No corresponding sequences in flies were identified for human Tuba. ND is not determined.

Table S2. List of primers and their sequence used in this study.

Sl.No.	PRIMER NAME	SEQUENCE
1	ICA69 FL Forward	5′-AAAGAATTCATGCTCAAGTCGGAGGTTCAGCACCAG-3′
2	ICA69 FL Reverse	5′-AAAGCGGCCGCTCAGGTCTGCTCGGCCACA-3′
3	ICA69 361aa Forward	5′-AAGAATTCATGCTCAAGTCGGAGGTT-3′
4	ICA69 361aa Reverse	5′-AAAAGCTTTCACTTCGAGTCCGTGGCT -3′
5	rp49 Forward	5′-GCCGCTTCAAGGGTGTCAGC-3′
6	rp49 Reverse	5′-CTTGCGCTTCTTGGAGGAGA-3′
7	ICA69 RT Forward	5′-CAATCGAAGCCGTGGATAAG-3′
8	ICA69 RT Reverse	5′-AAGCAAGGATTCATTGTCGC-3′
9	KO RT Forward	5′-CCAACCAAATTCGCCCAGTG-3′
10	KO RT Reverse	5′-CAGCTGACACACGGACTCAT-3′
11	ICA69 BAR KG Forward	5′-AAACTCGAGATGCTCAAGTCGGAGGTTCAGCACC -3′
12.	ICA69 BAR KG Reverse	5′-AAAAAGCTTTCAGGTCTGCTCGGCCACACT-3′
13.	ICA69 FL GW Forward	5′-CACCATGCTCAAGTCGGAGGTTCAG-3′
14.	ICA69 FL GW Reverse	5′-TCAGGTCTGCTCGGCCACACTGCGT-3′
15.	ICA69 BAR GW Reverse	5′-TCAGGCCTTAGATATGGTCTGGAAT-3′
16.	ICAC GW Forward	5′-CACCATGTTGATTATAAAGCCCAAG-3′

Table S3. Genotypes and NMJ morphology quantification at muscle 6/7 in abdominal segment A2. N represents the number of NMJ or the boutons used for quantification.

Genotype	NMJ length/Muscle area (μm^{-1})X10^3	Average bouton area (μm^2)	Bouton number/Muscle area	Total number of branches
Control	5.2 ± 0.5 N=14	8.0 ± 0.4 N=31	1.6 ± 0.2 N=14	11.9 ± 0.6 N=14
elav-Gal4>ICA69 RNAi	5.9 ± 0.1 N=14	7.9 ± 0.3 N=26	1.6 ± 0.1 N=14	12.4 ± 0.8 N=14
mef2-Gal4>ICA69 RNAi	4.9 ± 0.2 N=14	5.5 ± 0.4 N=30	0.9 ± 0.1 N=14	7.2 ± 0.5 N=14
Actin 5C-Gal4>ICA69 RNAi	4.9 ± 0.2 N=14	5.8 ± 0.4 N=31	0.9 ± 0.1 N=14	7.4 ± 0.5 N=14
GS13474/Df(3L)BSC553	5.9 ± 0.3 N=14	5.5 ± 0.4 N=31	0.7 ± 0.1 N=14	6.8 ± 0.5 N=14
GS14708/Df(3L)BSC553	4.9 ± 0.3N=14	5.5 ± 0.3 N=31	0.9 ± 0.1 N=14	7.5 ± 0.4 N=14
elav-Gal4/+;UAS-dICA69^{FL}/+; Df(3L)BSC553/GS13474	5.8 ± 0.1 N=14	5.7 ± 0.2 N=25	0.9 ± 0.1 N=14	7.9 ± 0.6 N=14
UAS-dICA69^{FL}/+; mef2-Gal4, Df(3L)BSC553/GS13474	5.5 ± 0.1 N=14	7.6 ± 0.6 N=31	1.6 ± 0.1 N=14	12.1 ± 0.7 N=14
UAS-dICA69^{FL}/+; Actin 5C-Gal4, Df(3L)BSC553/GS13474	5.4 ± 0.2 N=14	8.1 ± 0.5 N=31	1.6± 0.1 N=14	12.1± 0.8 N=14

Table S4. Genotypes and iGluR intensity quantification

Genotype	GluRIII intensity	GluRIIA intensity	GluRIIB intensity
Control	100.0 ± 4.3 N=50	100.0 ± 3.5 N=50	100.0 ± 3.9 N=50
Actin 5C-Gal4>ICA69 RNAi	62.4 ± 3.0 N=50	59.4 ± 2.3 N=50	62.7 ± 2.1 N=50
GS13474/Df(3L)BSC553	60.5 ± 2.1 N=50	57.1 ± 3.5 N=40	58.5 ± 3.6 N=50
elav-Gal4/+;UAS dICA69^{FL}/+; Df(3L)BSC553/GS13474	68.9 ± 1.9 N=40	66.1 ± 1.8 N=41	75.4 ± 3.3 N=40
UAS dICA69^{FL}/+; mef2-Gal4, Df(3L)BSC553/GS13474	92.4 ± 3.8 N=38	92.0 ± 7.4 N=40	91.5 ± 6.2 N=40
UAS dICA69^{FL}/+; Actin 5C-Gal4, Df(3L)BSC553/GS13474	91.4 ± 4.8 N=40	89.6 ± 4.9 N=40	90.9 ± 3.4 N=40
UAS dICA69^{FL}/+; mef2-Gal4/+	53.9 ± 4.9 N=41	40.1 ± 2.0 N=40	66.0 ± 2.6 N=50
mef2-Gal4>ICA69 RNAi	66.1 ± 1.9 N=39	59.5 ± 4.1 N=40	60.5 ± 3.1 N=50

Supplementary Materials and Methods

Generation of *Drosophila* ICA69 antibodies:

The antisera against *Drosophila* ICA69 were raised in rabbits against the N-terminal, 1-361 ($ICA69^{1-361}$) amino acids of ICA69. Nucleotide sequence corresponding to first 361 amino acids of ICA69 were amplified from cDNA, and cloned into the pET-28a (+) bacterial expression vector. Histidine-tagged recombinant protein ($His6\text{-}ICA69^{1-361}$) was expressed in BL21 CodonPlus bacterial cells, and purified from the inclusion bodies. In order to raise antibodies against ICA69, $His6\text{-}ICA69^{1-361}$ was mixed vigorously with an equal volume of complete Freund's adjuvant (Sigma) for emulsion formation. About 200 µg of emulsified protein was injected into each of the two rabbits used for antisera generation (Deshpande Laboratories, Bhopal, India). Four booster dose were given with 100 µg of protein in incomplete Freund's adjuvant at two-week intervals. The serum was separated from the blood collected through ear bleeding. The ICA69 antibodies were affinity purified from the serum, and its specificity was confirmed by performing immunostaining and Western blot (Fig. 2A-C).

Immunocytochemistry

Wandering third instar larvae were dissected on a sylgard dish in cold calcium-free HL3 saline and fixed in 4% paraformaldehyde in PBS for 30 minutes or in Bouin's fixative (GluRIIA staining) for 5 minutes. Larval fillets were then washed in PBS containing 0.2% Triton X-100, blocked for one hour in 5% normal goat serum, and then incubated overnight at 4°C with the primary antibody. The anti-ICA69 antibody was used at 1:600 dilution for immunostaining. Monoclonal antibodies: anti-Dlg (4F3), anti-DGluRIIA (8B4D2), anti-CSP (ab49), anti-Synapsin (3C11), anti-actin (JLA20) and anti-α-Spectrin (3A9) were obtained from the Developmental Studies Hybridoma Bank (University of Iowa, USA) and were used at 1:50 dilution. Anti-GluRIIB (1:1000) (Marrus and DiAntonio, 2004) and GluRIII (1:5000) (Marrus et al., 2004) were gifts from Aaron DiAntonio (Washington University, St. Louis,

USA). Wasp (1:200) (Bogdan et al., 2005) and SCAR (1:50) (Zallen et al., 2002) antibodies were a gift from Sven Bogdan (University of Munster, Germany) and Eyal Schejter (Weizmann Institute of Science, Israel) respectively. Fluorophore coupled secondary antibodies Alexa Fluor 488, Alexa Fluor 568 or Alexa Fluor 633 (Molecular Probes, Thermo Fisher Scientific) were used at 1:800 dilution. DAPI and Alexa 488-conjugated anti-HRP were used at 1:2000 and 1:800 dilutions respectively. Stained larval preparations were mounted in VECTASHIELD (Vector Laboratories, USA) and imaged with a laser scanning confocal microscope (LSM 780; Carl Zeiss). All the images were processed with Adobe Photoshop 7.0 (Adobe Systems, San Jose, CA).

Supplementary Figures

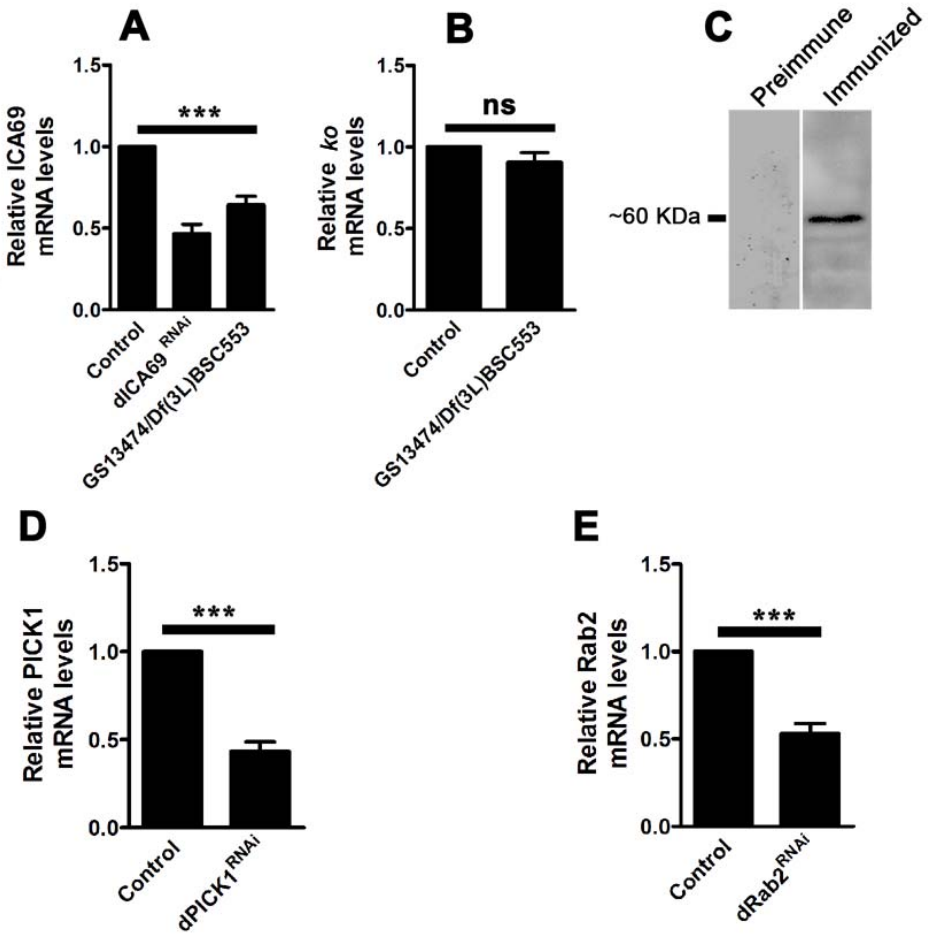

Figure S1. Characterization of hemizygous *ICA69* mutant and Western blot using ICA69 antibody. (A-B) Quantitative RT-PCR showing transcript levels of *ICA69* in controls, *Actin 5C*-Gal4 driven *ICA69* RNAi and hemizygous *ICA69* mutant (*GS13474/Df(3L)BSC553*), respectively. *ICA69* transcript levels were significantly reduced in *Actin 5C*-Gal4 driven *ICA69* RNAi and *ICA69* hemizygous mutant. Expression level of the neighboring upstream gene, *ko* remains unaltered in hemizygous mutant. *rp49* transcript level was used as an internal expression control. (C) Western blot showing that polyclonal ICA69 antibody detects a single band of about 60 kDa in *Drosophila* fillet lysates. About 300 µg

protein was loaded in each lane. The preimmune serum does not detect any band in the lysate. (D) Quantitative RT-PCR depicting transcript levels of *PICK1* in controls and *Actin 5C* -Gal4 driven *PICK1* RNAi. Compared to control, *Actin 5C*-Gal4 driven *PICK1* RNAi led to ~60% reduction in *PICK1* transcript level. (E) Quantitative RT-PCR depicting transcript levels of *Rab2* in controls and *Actin 5C*-Gal4 driven *Rab2* RNAi. Compared to control, *Actin 5C*-Gal4 driven *Rab2* RNAi led to ~50% reduction in *Rab2* transcript level. Error bars represent mean±s.e.m. ***p < 0.0001; ns, not significant. Statistical analysis based on one-way ANOVA with post-hoc Tukey's test for multiple comparisons.

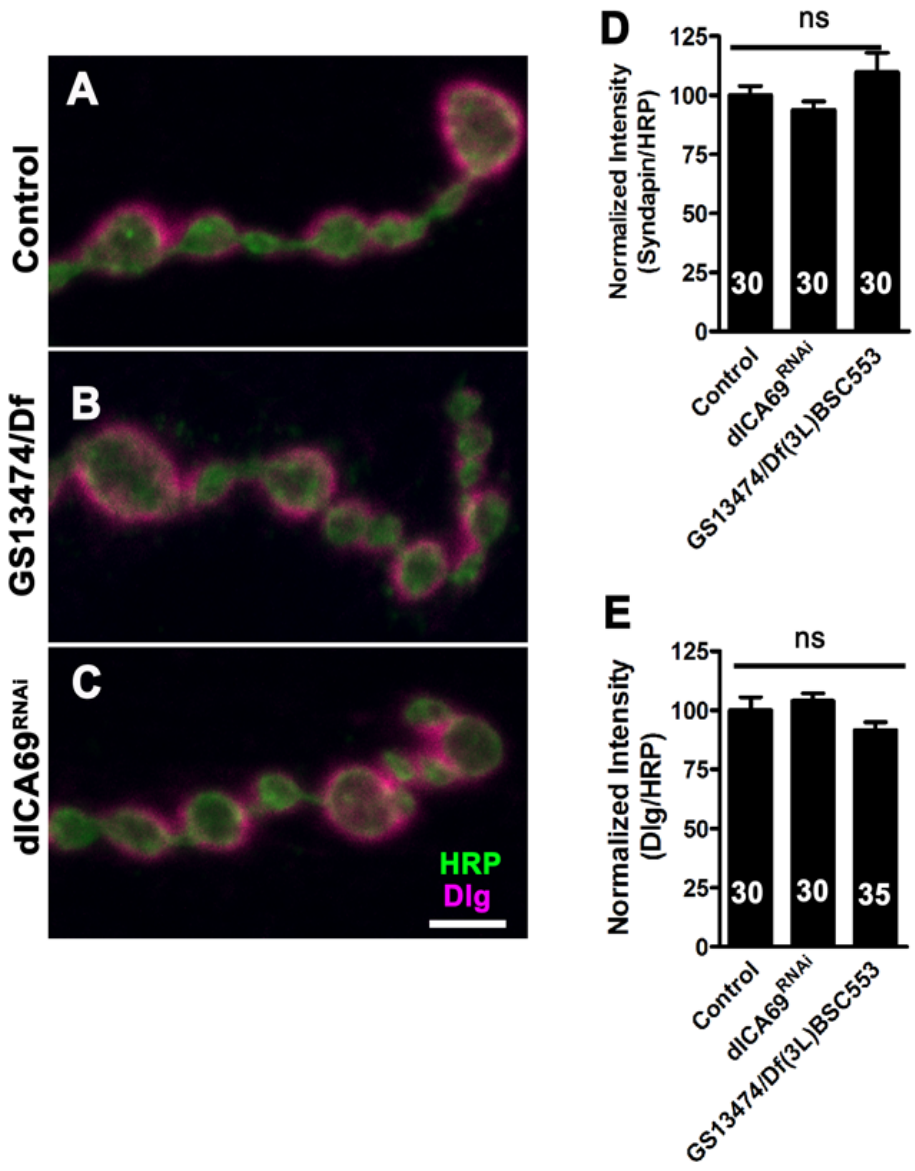

Figure S2. Synaptic level of Dlg and Syndapin remain unaltered in *ICA69* mutant. (A-C) Confocal images of boutons at third instar larval NMJ synapse in (A) Control, (B) hemizygous *ICA69* mutant *(GS13474/Df(3L)BSC553*) and (C) *Actin 5C*-Gal4 driven *ICA69* RNAi double immunolabeled with anti-HRP (green) and anti-Dlg (magenta). Note that the gross morphology of SSR and the immunoreactivity of Dlg remain unaltered in *ICA69* hemizygous mutant and RNAi depleted animals. Scale bar represents 10 µm. (D) Histogram showing normalized synaptic fluorescence level of Syndapin in control, *Actin 5C*-Gal4 driven *ICA69* RNAi and *GS13474/Df(3L)BSC553* hemizygous *ICA69* mutant. (E) Histogram

showing normalized synaptic fluorescence level of Dlg in control, *Actin 5C*-Gal4 driven *ICA69* RNAi and *GS13474/Df(3L)BSC553* hemizygous mutant. Error bars represent mean±s.e.m. ns, not significant. Statistical analysis based on one-way ANOVA with post-hoc Tukey's test for multiple comparisons.

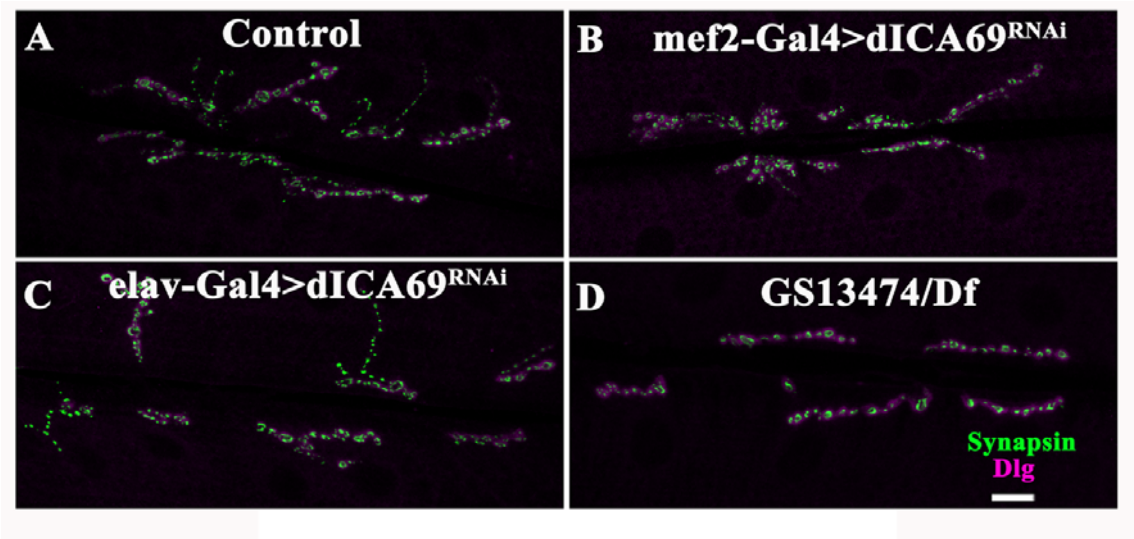

Genotypes	No. of NMJ analyzed	No. of footprints
Control	30	2
mef2-Gal4>dICA69 RNAi	25	2
elav^{C155}-Gal4>dICA69 RNAi	30	3
GS13474/Df(3L)BSC553	25	1

Figure S3. Knockdown of ICA69 either in neurons or muscles does not affect synapse retraction. Confocal images of NMJ synapse at muscle 6/7 of **(**A) Control, (B) *mef2*-Gal4 driven *ICA69* RNAi (C) *elav^{C155}*-Gal4 driven *ICA69* RNAi, and (D) *GS13474/Df (3L)BSC553* double immunolabeled with anti-Synapsin (green) and anti-Dlg (magenta). The Dlg immunostaining tightly associates with Synapsin staining, suggesting normal synapse stability in these genotypes. The lower panel shows the quantification of retracted boutons in the indicated genotypes.

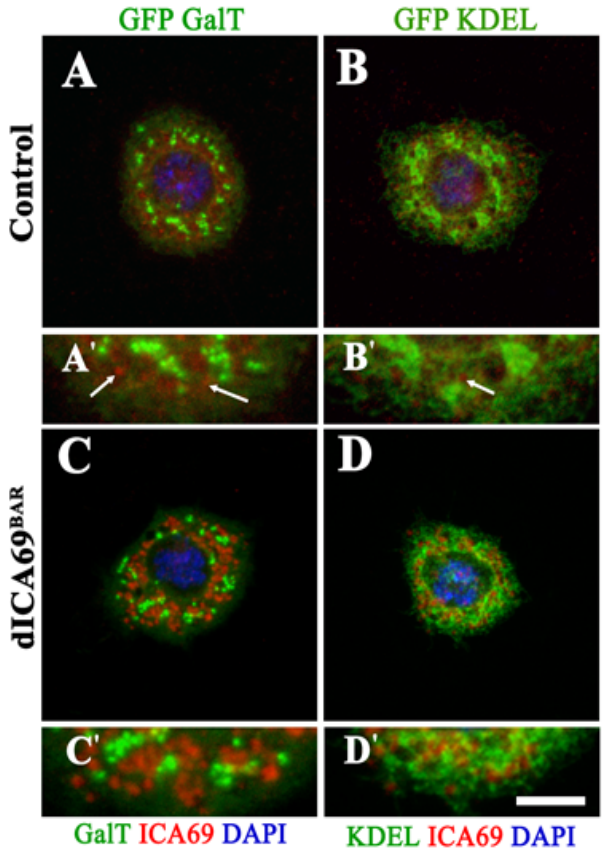

Figure S4. ICA69 does not colocalize with known markers of Golgi or endoplasmic reticulum in S2R+ cells. (A-B) Confocal images of S2R+ cells transfected with either GFP-GalT or GFP-KDEL and immunostained with anti-ICA69 antibodies. A portion of the stained image is shown as enlarged image in A' and B'. Endogenous ICA69 does not colocalize with either Golgi (marked by GFP-GalT) or ER (marked by GFP-KDEL). *Drosophila* ICA69 is localized around the cell nuclei, and a fraction of it exists as small foci (marked by arrow). (C-D) Confocal images of S2R+ cells cotransfected with ICA69-BAR and (C) GFP-GalT or (D) GFP-KDEL and immunostained with anti-ICA69 antibodies. A portion of the stained image is shown as enlarged image in C' and D'. Expression of ICA69-BAR domain induces the formation of structures which appear like vesicles. These structures

do not colocalize with either Golgi or ER. The nature of these structures remains to be determined. Scale bar represents 10 µm for (A-D) and 4 µm for (A'-D').

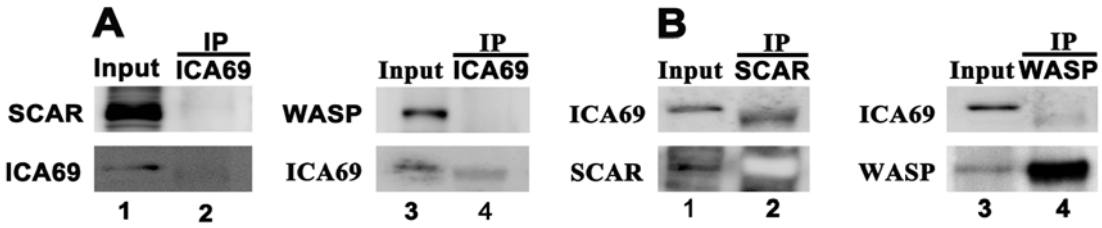

Figure S5. ICA69 does not directly associate with Wasp or SCAR. (A) Anti-ICA69 antibody was used to pull-down SCAR or Wasp from the fly head lysates. The immune complexes, and the input were analyzed by immunoblotting using antibodies specific to SCAR (upper panel, lane 1-2) or Wasp (upper panel lane 3-4). Same samples were used to detect ICA69 (Lower panel, 1-4). Endogenous SCAR and Wasp does not precipitate with ICA69. (B) Reciprocal Co-Immunoprecipitation (Co-IP) with anti-SCAR and anti-Wasp antibodies. Immune complexes and input were analyzed by immunoblotting with anti-ICA69 (upper panel, lane 1-2 and 3-4 respectively). Same samples were used to analyze SCAR and Wasp (lower panel, 1-2 and 3-4 respectively). SCAR and Wasp do not interact with ICA69 whereas SCAR and Wasp are detectable in the pull-down sample.

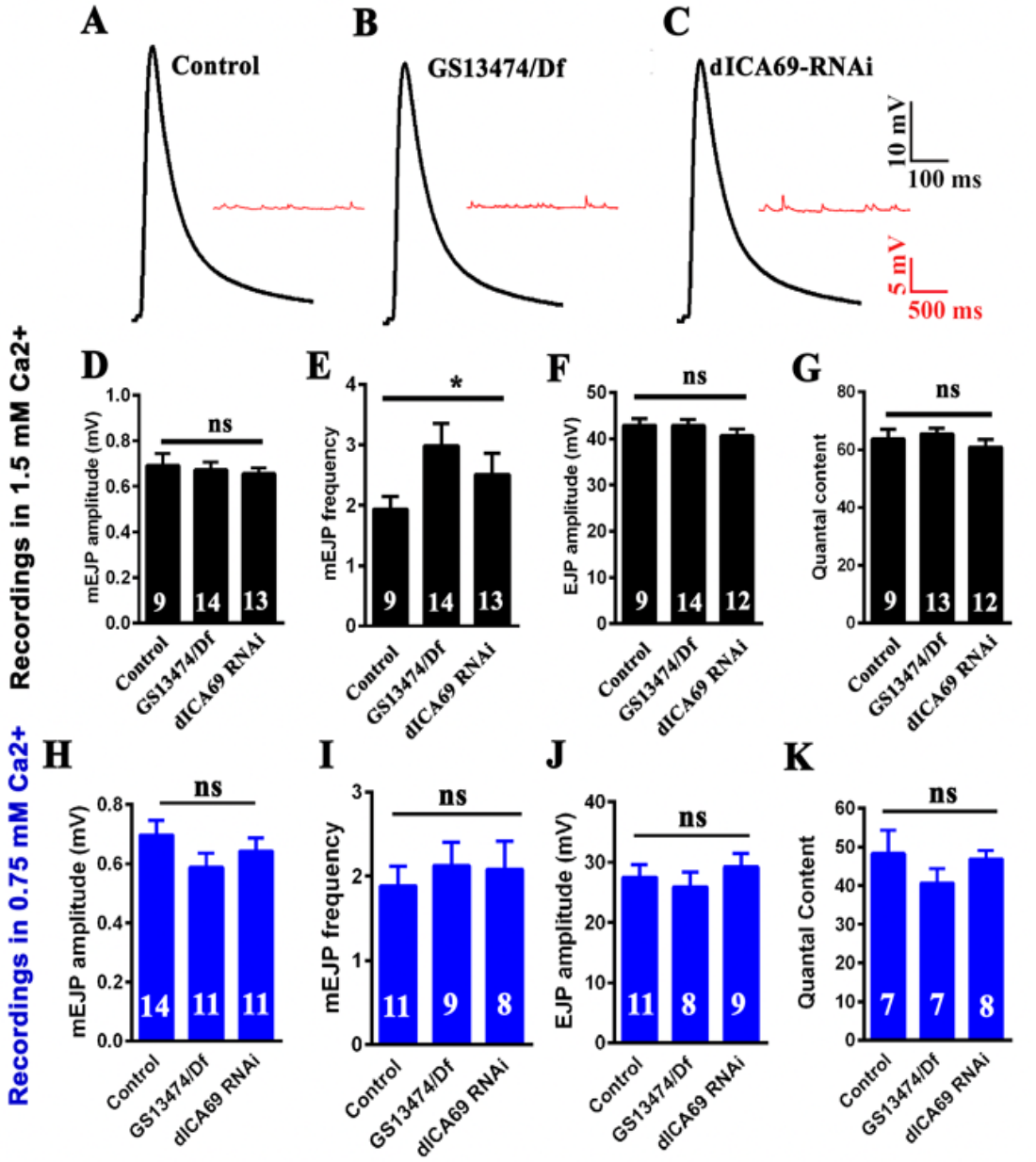

Figure S6. *ICA69* mutant show normal synaptic physiology. (A-C) Representative traces of evoked junction potentials (thick black traces) or miniature junction potentials (red traces) in control, hemizygous *ICA69* mutant combinations (*GS13474/Df(3L)BSC553*) and *Actin 5C*-Gal4 driven *ICA69* RNAi animals. (D) Histograms showing average mEJP amplitude in control (0.69 ± 0.05 mV), hemizygous *ICA69* mutant combinations (*GS13474/Df(3L)BSC553,* 0.67 ± 0.03 mV) and *Actin 5C* -Gal4 driven *ICA69* RNAi (0.65 ± 0.02 mV) animals. The number in the columns represents the number of NMJ recordings of each genotype. (E) Histograms showing average mEJP frequency in control (1.93 ± 0.2),

hemizygous *ICA69* mutant combinations (*GS13474/Df(3L)BSC553*, 2.98 ± 0.37) and *Actin 5C*-Gal4 driven *ICA69* RNAi (2.5 ± 0.35) animals. The number in the column represents the number of NMJ recordings of each genotype. (F) Histograms showing average EJP amplitude in control (42.89 ± 1.41 mV), hemizygous *ICA69* mutant combinations (*GS13474/Df(3L)BSC553*, 42.82 ± 1.33 mV) and *Actin 5C*-Gal4 driven *ICA69* RNAi (40.65 ± 1.42 mV) animals. The number in the column represents the number of NMJ recordings of each genotype. (G) Histograms showing average quantal content in control (63.64 ± 3.34), hemizygous *ICA69* mutant combinations (*GS13474/Df(3L)BSC553*, 65.38 ± 2.11) and *Actin 5C*-Gal4 driven *ICA69* RNAi (60.90 ± 2.62) animals. The number in the columns represents the number of NMJ recordings of each genotype. These recordings were performed in 1.5 mM Ca^{2+} concentration. (H-K) Represents quantification of mEJP amplitude, mEJP frequency, EJP amplitude and the quantal content in control, hemizygous *ICA69* mutant (*GS13474/Df(3L)BSC553*) and *Actin5C*-Gal4 driven *ICA69* RNAi animals. These recordings were performed in 0.75 mM Ca^{2+} concentration. Error bars represent mean±s.e.m. *$p < 0.01$; ns, not significant. Statistical analysis based on one-way ANOVA with post-hoc Tukey's test for multiple comparisons.

SUPPLEMENTAL REFERENCES

Bogdan, S., Stephan, R., Lobke, C., Mertens, A., and Klambt, C. (2005). Abi activates WASP to promote sensory organ development. Nat Cell Biol *7*, 977-984.

Marrus, S.B., and DiAntonio, A. (2004). Preferential localization of glutamate receptors opposite sites of high presynaptic release. Curr Biol *14*, 924-931.

Marrus, S.B., Portman, S.L., Allen, M.J., Moffat, K.G., and DiAntonio, A. (2004). Differential localization of glutamate receptor subunits at the Drosophila neuromuscular junction. J Neurosci *24*, 1406-1415.

Zallen, J.A., Cohen, Y., Hudson, A.M., Cooley, L., Wieschaus, E., and Schejter, E.D. (2002). SCAR is a primary regulator of Arp2/3-dependent morphological events in Drosophila. J Cell Biol *156*, 689-701.